Self-Standing End-Fed Electrically Quasi-Uniform Linear Arrays: Analysis, Design, Construction, Measurements and FLOSS

K.Th. Kondylis, N.I. Yannopoulou, P.E. Zimourtopoulos *

Antennas Research Group, Athens, Greece [1]
Antennas Research Group, Austria [2, 3]

Abstract

Based on the analysis presented by the authors in their previous work for end-fed space arrays, where an application to geometrically uniform self-standing linear arrays of parallel dipoles was given, this paper presents the results of a single driving-point, self-standing, fully uniform linear array, that is one which has electrical uniformity, as well as, an application to the constrained pattern design. During the synthesis process and due to the multiplicity of solutions resulting from the complex analytical relations given here, the criterion of Electrically Quasi-Uniform Linear Array EQ-ULA was introduced. An experimental array model was designed, simulated, constructed, and its three main-plane radiation patterns were measured. The measurements were found in good agreement with analytical, computational, and theoretical results, and thus the proposed technique was experimentally proved. The developed software applications are available as FLOSS Free Libre Open Source Software.

Keywords

End-fed, single driving-point, self-standing arrays

Introduction

Fully Uniform Linear Arrays ULA are both geometrically GULA and electrically EULA uniform i.e. the dipoles are equidistant with consecutive dipole currents equal in amplitude and of constant phase difference, respectively [1]. The complex vector radiation pattern of such an array is E = AG where G is the Generator Pattern, and A is the Array Factor i.e. the complex numerical radiation pattern of N invented isotropic point sources, each of current I_k and pointed by the dipole center vector R_k. Linear Arrays are those which have their corresponding point sources on a straight line.

Using the relations for end-fed, single driving-point, self-standing linear arrays presented in the previous author's work [2], where only the first condition of geometrical uniformity was imposed, the case of a fully ULA is examined here. Due to increasing complexity of current expressions with number of dipoles and for all other reasons that were detailed in [2], the ULA procedure is applied just for the simplest, next to trivial, linear array of three dipoles shown in Fig. 1.

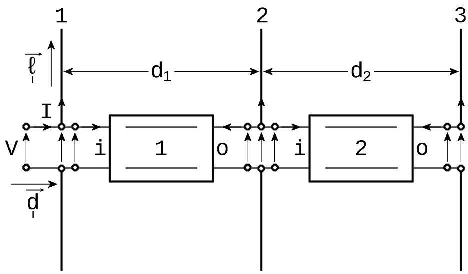

Fig. 1: End-fed linear array of 3 linear dipoles

Analysis

By applying the analysis presented in previous work [2] for $N = 3$ dipoles, $6N - 3 = 15$ linear relations between $6N - 2 = 15$ variables + 1 parameter, the source voltage V, result, as shown in Fig. 2 in a compact form when $\beta\ell_1$, $\beta\ell_2 \neq \nu\pi$, $\nu = 1, 2, \ldots$ for both transmission lines, with each cell value to be the coefficient of the variable in the first row of its column in an implied summation. For the case of $\beta\ell_1 = \nu\pi$, $\nu = 1, 2, \ldots$ the two upper gray rows have to be substituted by the rows of Fig. 3 or 4, according to the odd or even value of ν and similarly, if $\beta\ell_2 = \nu\pi$, $\nu = 1, 2, \ldots$ the two last gray rows have to be substituted by those of Fig. 5 or 6.

The equivalent circuit is shown in Fig. 7. The GUI application form for the computation of current ratios of $N = 3$ dipoles, developed with Visual Fortran, is given in Fig. 8 [3], [4]. In this form, the input data are: the distances between dipoles, the dipole radius and length, the length, the characteristic impedance Z_0, and the velocity factor vf of each transmission line segment. In addition to current ratios, the application exports the text files needed by the [RadPat4W] application of the RGA FLOSS mini-Suite of tools [5]. The formulas for the determination of the $1 + 2 = 3$ current ratios (I_k/I_1) were mechanically verified using Mathematica. The expressions of the two current ratios (I_2/I_1, I_3/I_1) of the GUI are given by (1)-(5) below:

V_1	V_2	V_3	I_1	I_2	I_3	${}_iV_1$	${}_oV_1$	${}_iI_1$	${}_oI_1$	${}_iV_2$	${}_oV_2$	${}_iI_2$	${}_oI_2$	I	=	V
1															=	1
1						−1									=	0
			1					1						−1	=	0
	1									−1					=	0
	1						−1								=	0
				1					1			1			=	0
		1									−1				=	0
					1								1		=	0
−1			Z_{11}	Z_{12}	Z_{13}										=	0
	−1		Z_{21}	Z_{22}	Z_{23}										=	0
		−1	Z_{31}	Z_{32}	Z_{33}										=	0
						−1		${}_{ii}Z_1$	${}_{io}Z_1$						=	0
							−1	${}_{oi}Z_1$	${}_{oo}Z_1$						=	0
										−1		${}_{ii}Z_2$	${}_{io}Z_2$		=	0
											−1	${}_{oi}Z_2$	${}_{oo}Z_2$		=	0

Fig. 2: The linear system of 15 relations for arrays with $N = 3$ and $\beta\ell_1$, $\beta\ell_2 \neq \nu\pi, \nu = 1, 2, \ldots$

						1	1								=	0
								−1	1						=	0

Fig. 3: 2 upper gray rows for $\nu = 2\mu + 1$, $\mu = 0, 1, 2, \ldots$

						−1	1								=	0
								1	1						=	0

Fig. 4: 2 upper gray rows for $\nu = 2\mu + 2$, $\mu = 0, 1, 2, \ldots$

										1	1				=	0
												−1	1		=	0

Fig. 5: 2 last rows replacement for $\nu = 2\mu + 1$, $\mu = 0, 1, 2, \ldots$

										−1	1				=	0
												1	1		=	0

Fig. 6: 2 last rows replacement for $\nu = 2\mu + 2$, $\mu = 0, 1, 2, \ldots$

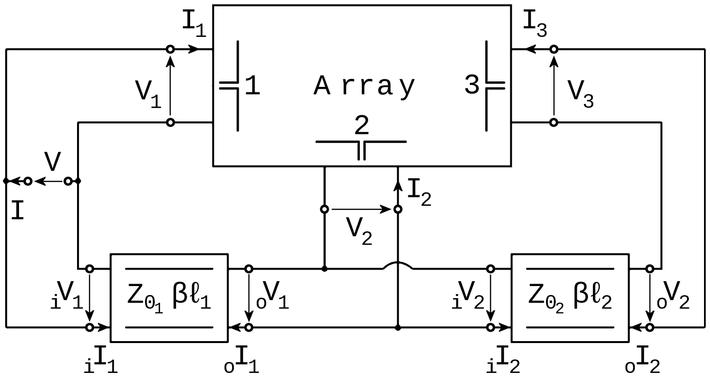

Fig. 7: Equivalent circuit of the 3 dipoles linear array

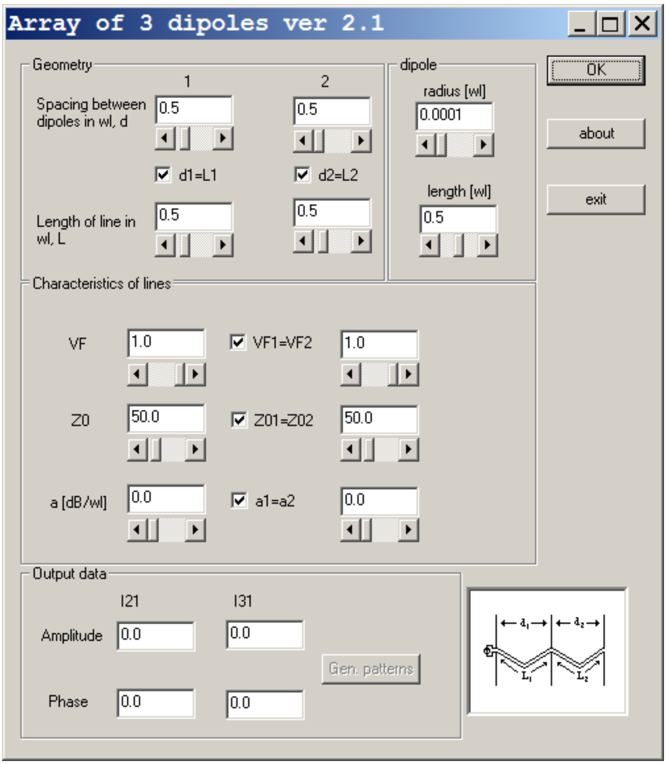

Fig. 8: GUI for the analysis of a linear array

of $N = 3$ dipoles

$$I_{21} = \frac{I_2}{I_1} = \frac{A_{21}}{P} \quad (1)$$

$$I_{31} = \frac{I_3}{I_1} = \frac{A_{31}}{P} \quad (2)$$

$$\begin{aligned} A_{21} = {} & \left[{}_{io}z_2\left(z_{11} z_{23} - z_{12} z_{13}\right) + {}_{ii}z_2\left(z_{13}^2 - z_{11}^2\right)\right]{}_{io}z_1 + \\ & + \left(z_{11} z_{12} - z_{13} z_{23}\right){}_{ii}z_1\, {}_{ii}z_2 + \\ & + \left[z_{12}\left(z_{11} + {}_{ii}z_2\right) - z_{13}\left(z_{23} + {}_{io}z_2\right)\right]\left({}_{ii}z_1^2 - {}_{io}z_1^2\right) - \\ & - \left(z_{11}\, {}_{io}z_1 - z_{12}\, {}_{ii}z_1\right)\left({}_{ii}z_2^2 - {}_{io}z_2^2\right) \end{aligned} \quad (3)$$

$$\begin{aligned} A_{31} = {} & \left[{}_{io}z_2\left(z_{12}^2 - z_{11}^2\right) + {}_{ii}z_2\left(z_{11} z_{23} - z_{12} z_{13}\right)\right]{}_{io}z_1 + \\ & + \left(z_{11} z_{13} - z_{12} z_{23}\right){}_{ii}z_1\, {}_{ii}z_2 + \\ & + \left[z_{13}\left(z_{11} + {}_{ii}z_2\right) - z_{12}\left(z_{23} + {}_{io}z_2\right)\right]\left({}_{ii}z_1^2 - {}_{io}z_1^2\right) \end{aligned} \quad (4)$$

$$\begin{aligned} P = {} & \left[{}_{io}z_2\left(z_{11} z_{13} - z_{12} z_{23}\right) + {}_{ii}z_2\left(z_{11} z_{12} - z_{23} z_{13}\right)\right]{}_{io}z_1 + \\ & + \left(z_{11}^2 + z_{23}^2\right){}_{ii}z_1\, {}_{ii}z_2 - \\ & - \left[\left(z_{11} + {}_{ii}z_2\right)^2 + \left(z_{23} + {}_{io}z_2\right)^2\right]\left({}_{ii}z_1^2 - {}_{io}z_1^2\right) + \\ & + \left(z_{12}\, {}_{io}z_1 - z_{11}\, {}_{ii}z_1\right)\left({}_{ii}z_2^2 - {}_{io}z_2^2\right) \end{aligned} \quad (5)$$

in which the equality of self and mutual impedances resulting from the system of Fig. 2, have been taken into account.

ULA Synthesis and Design

The simplest end-fed linear array of three dipoles is the one with the interelement distance equal to the transmission line length. Fig. 9 shows the two amplitude current ratios for a two-wire transmission line of $Z_0 = 200\ \Omega$ and $vf = 1$, and Fig. 10 the phase difference between the consecutive dipoles, in terms of the s/λ distance, with minimum value 0.005 and maximum 1. The two conditions imposed by EGULA or simply ULA are:

$$\left|\frac{I_3}{I_1}\right| = \left|\frac{I_2}{I_1}\right| = 1, \quad \measuredangle\frac{I_2}{I_1} = \measuredangle\frac{I_3}{I_2} = \alpha \quad (6)$$

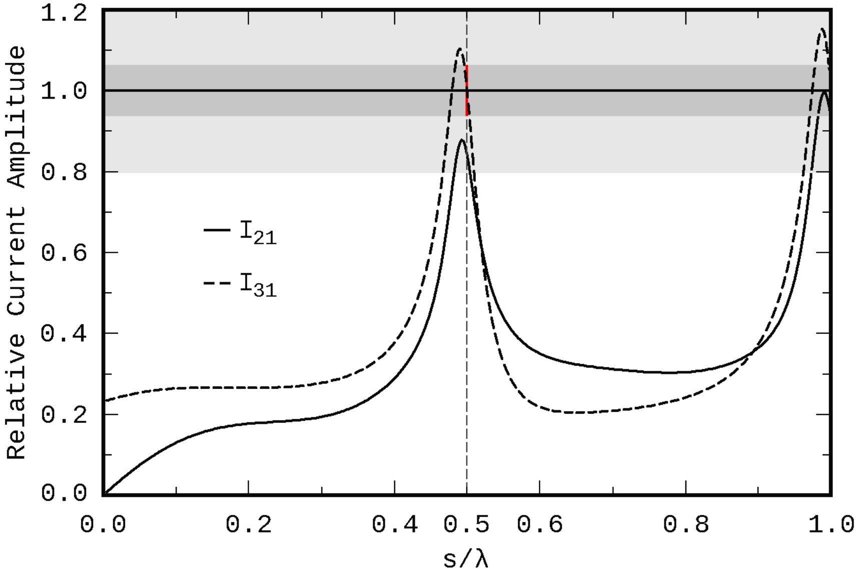

Fig. 9: Amplitude of current ratios for $s = d = \ell$

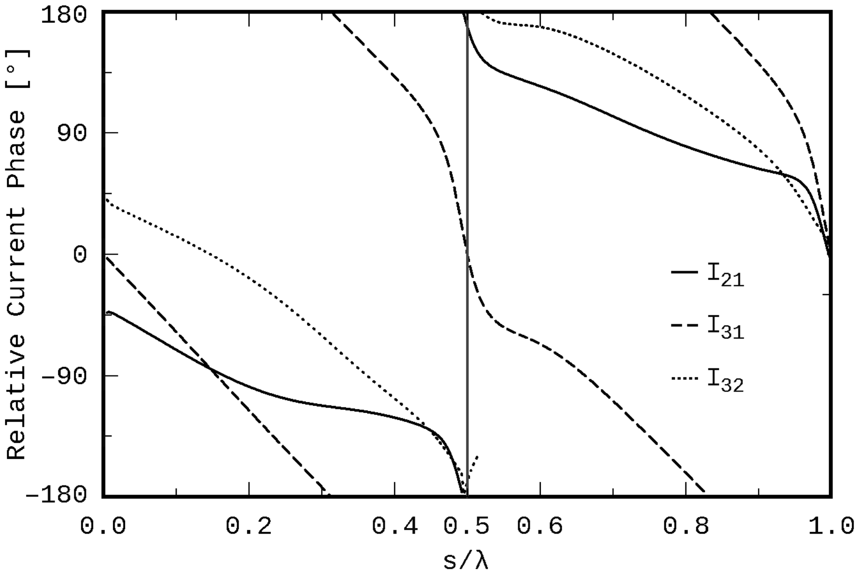

Fig. 10: Phase difference of current ratios for $s = d = \ell$

The value of $s = 0.5\lambda$ was selected as the most probable to produce an ULA. The other possible value of s is near 1λ and leads to long distanced dipoles which are not mechanically suitable for an end-fed array. From these figures it is obvious that there is no uniform linear array which is ULA, with $s = d_1 = d_2 = \ell_1 = \ell_2$, even by considering a ±6% variation from the desired value of the current ratios, as it is shown with the dark gray frame in Fig. 9. The only one array that could be an ULA, is the one with current ratio values which may be within the large light gray frame in Fig. 9, that is of a ±20% margin around 1, corresponding to the rather trivial case of an ULA with phase difference ±180°, as this is indicated by the vertical dark gray line in Fig. 10.

Since the main purpose was to investigate the possibility of design, build and measure an end-fed self-standing ULA for use in practical applications, where just a few pattern constraints are imposed, the synthesis procedure is applied to the case of the 3 dipoles array.

Let suppose that it is required that the array factor A has a minimum in the direction of 45° and a maximum in 135° from the array axis, as shown in Fig. 11, where $\mathcal{A}$ is the normalized array factor and $\xi_d \in [0, \pi]$ is the angle from the array axis to any direction.

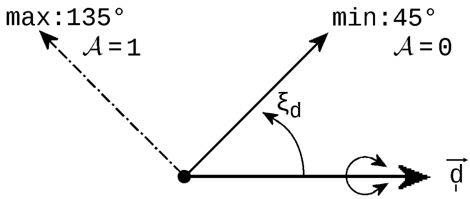

Fig. 11: Directions of $\mathcal{A}$ minimum and maximum

According to the above theory, the following two parameters define the ULA of 3 dipoles: constant phase difference α between consecutive dipoles and equidistance d/λ, as they are given by (6). There are two equivalent techniques to determine these two parameters:

i) the algebraic one, which involves the solution of a number of 2x2 systems of linear equations:

$$\begin{bmatrix} \cos\xi_d^a & 1 \\ \cos\xi_d^b & 1 \end{bmatrix} \begin{bmatrix} \beta d \\ \alpha \end{bmatrix} = \begin{bmatrix} \psi^a \\ \psi^b \end{bmatrix}, \ \xi_d^a \neq \xi_d^b \Rightarrow$$

$$\beta d = \frac{\psi^a - \psi^b}{\cos\xi_d^a - \cos\xi_d^b}$$
$$\alpha = \frac{\psi^b \cos\xi_d^a - \psi^a \cos\xi_d^b}{\cos\xi_d^a - \cos\xi_d^b} \qquad (7)$$

ii) the geometric technique of uniform array synthesis [1 p. 45].

Both of them are based on the periodic function:

$$\mathcal{A}(\psi) = \frac{1}{N}\left|\frac{\sin\left(\frac{N\psi}{2}\right)}{\sin\left(\frac{\psi}{2}\right)}\right| \quad (8)$$

where $\psi = \beta d\cos(\xi_d) + \alpha$ with primary interval $(-\pi, \pi]$. $\mathcal{A}(\psi)$ is drawn as in Fig. 12(a). The points on ψ axis give minimum (zero) values of $\mathcal{A}$.

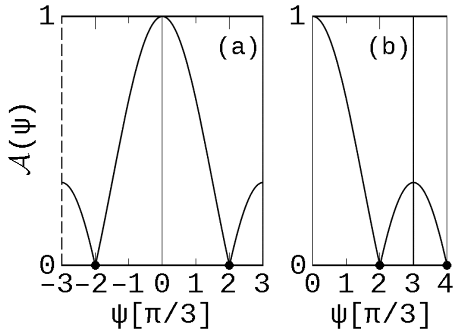

Fig. 12: ULA Array Factor $\mathcal{A}$

Using the algebraic technique, the principal interval is searched for possible solutions first. Since $\psi^a = 0$ in our case, and

$$\cos\xi_d^a - \cos\xi_d^b = \cos\frac{3\pi}{4} - \cos\frac{\pi}{4} = $$
$$= -\frac{\sqrt{(2)}}{2} - \frac{\sqrt{(2)}}{2} = -\sqrt{(2)}$$

the solutions (7) are of the form

$$\beta d = \frac{\psi^b}{\sqrt{(2)}}, \quad \alpha = \frac{\psi^b}{2} \quad (9)$$

Therefore, the first zero of $\mathcal{A}$ at $\psi^b = -2\pi/3$ is rejected, because it results in a negative distance, as well as at any other negative ψ, while the second one at $\psi^b = 2\pi/3$ gives

$$\beta d = \frac{2\pi}{3\sqrt{(2)}}, \quad \alpha = \frac{\pi}{3} \Rightarrow$$

$$\Rightarrow d \simeq 0.25\lambda, \quad \alpha = 60° \quad (10)$$

But, since this d value is only the half of $s = 0.5\lambda$, another one solution is sought at $\psi^b = 4\pi/3$ in the extended interval to the positive ψ axis, as shown in Fig. 12(b). Hence, a third 2x2 system as (7) is formed with solution

$$\beta d = \frac{4\pi}{3\sqrt{(2)}}, \quad \alpha = \frac{2\pi}{3} \Rightarrow$$

$$\Rightarrow d \simeq 0.5\lambda, \quad \alpha = 120° \quad (11)$$

in practice. This is the chosen solution and thus we have to look for a linear array of $N = 3$ dipoles $d = 0.5\lambda$ apart and with $\alpha = 120°$ phase difference.

After that, we successfully checked the above results by applying the geometric technique (ii), as it is shown in Fig. 13, where ψ_{max} is always equal to 0:

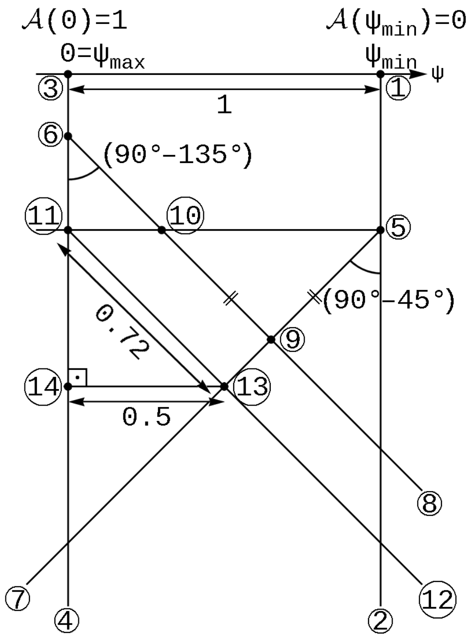

Fig. 13: Geometric technique

if $\mathcal{A}(\psi_{min}) = 0$ at $\psi_{min} = 2\pi/3$:

$$\beta d = |13-11| = 0.72\frac{2\pi}{3} \Rightarrow d \simeq 0.25\lambda$$

$$\alpha = |13-14| = 0.50\frac{2\pi}{3} \Rightarrow \alpha = 60°$$

as in (10) and at $\psi_{min} = 4\pi/3$:

$$\beta d = |13-11| = 0.72\frac{4\pi}{3} \Rightarrow d \simeq 0.5\lambda$$

$$\alpha = |13-14| = 0.50\frac{4\pi}{3} \Rightarrow \alpha = 120°$$

that is, the above solution (11).

This solution must satisfy the strict ULA requirements by using two segments of 200 [Ω] transmission line with appropriate length [2]. In practice, it is almost impossible to compromise all these analytical facts, since this issue is rather a matter of chance.

EQ-ULA design

In order to handle this practical problem we had the idea to somehow relax the ULA conditions by introducing the definition of the Electrically Quasi-Uniform Linear Array EQ-ULA as one with deviations ±ε and ±δ to ULA conditions of unity 1 and α of (6). The ε, δ design criteria will be defined by the user as in the following.

A Visual Fortran application [SYN3DIP] was developed in order to support this definition for the case of $N = 3$ dipoles, as shown in Fig. 14. The results of array synthesis are the input into the first frame, that is, the distance per wavelength d [wl] and the current phase difference in degrees α [deg] between successive dipoles. The next two frames correspond to the transmission line segments, which may have different or the same Z_0 and there is the possibility to search between an initial and final value of Z_0 with a specified step. The deviation margins, are given in the last frame, and their initial values for this EQ-ULA were chosen as $\varepsilon = \pm 20\%$, and $\delta = \pm 10°$.

The program execution results more than hundred (100) combinations of $\beta\ell_1$, $\beta\ell_2$ in [°] satisfying these two criteria. Fig. 15 shows the processed results from [SYN3DIP] where the minimum and maximum value of $\beta\ell_2$ are given inside each bar for every value of $\beta\ell_1$. Amplitude and phase difference are given in Fig. 16 and Fig. 17 respectively. From these figures, it is obvious that the most possible solutions are between 198 and 202 for $\beta\ell_1$. The value $\beta\ell_1 = 200°$ was selected and the relative complex currents I_{21}, I_{32} and I_{31} are plotted on the complex plane with $\beta\ell_2$ as parameter in Fig. 18. The shown outer and inner circle corresponds to the initial ε value and the outer most radials to the initial δ value with light gray color.

Attempting to further reduce the number of possible solutions the following more strict design margins were adopted: $\varepsilon = \pm 6\%$ and $\delta = \pm 2°$, shown with dark gray color regions in Fig. 18. Rerunning [SYN3DIP] a unique solution of $\beta\ell_2 = 307°$ has been achieved. In this manner, two line segments of different length resulted which exceed the dipoles equal distances of 0.5λ: $\ell_1 = 0.556\lambda$, $\ell_2 = 0.853\lambda$. Remarkably, the relative currents have almost unit amplitude and almost equal phase differences, that is, an almost ULA, an EQ-ULA.

Therefore, there is indeed a unique practical array, with the characteristics of Tab. 1 to solve the problem of designing an end-fed EQ-ULA capable to satisfy the imposed pattern constrains.

Tab. 1: Characteristics and current ratios of EQ-ULA

f	1111 [MHz]		N	3		
L	0.5λ	13.5 [cm]	Min	45°	Max	135°
d	0.5λ	13.5 [cm]	Z_0	200 [Ω]	vf	1
ℓ_1	0.556λ	15 [cm]		ℓ_2	0.853λ	23 [cm]
	$\lvert I_2/I_1\rvert$	$\lvert I_3/I_1\rvert$	$\lvert I_3/I_2\rvert$	$\measuredangle I_2/I_1$	$\measuredangle I_3/I_1$	$\measuredangle I_3/I_2$
	1.058	0.956	0.904	120.4°	−118.8°	120.8°

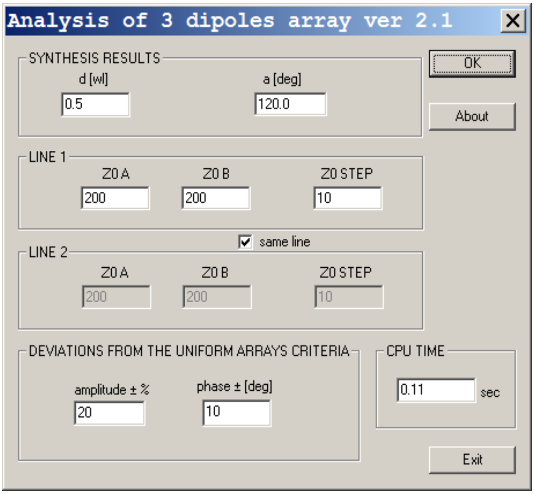

Fig. 14: GUI for Quasi-Uniform Array of $N = 3$ dipoles

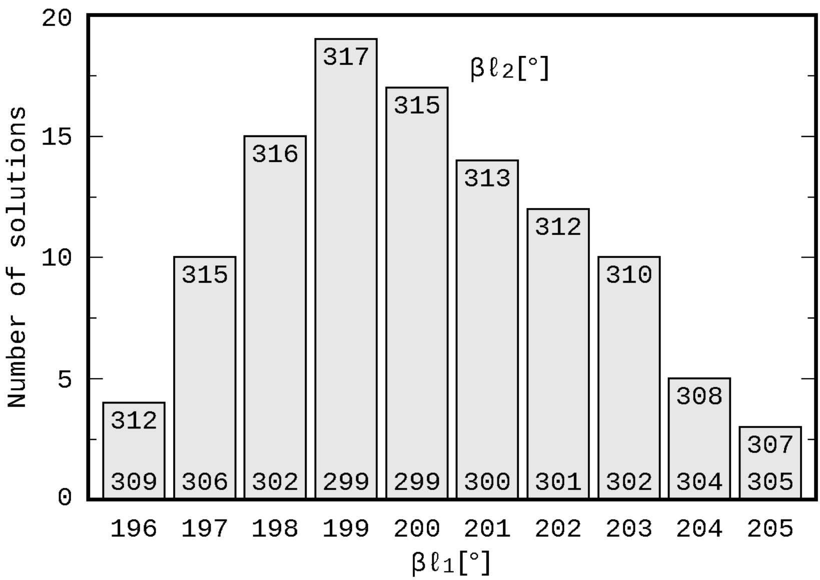

Fig. 15: Possible combinations of $\beta\ell_1$, $\beta\ell_2$

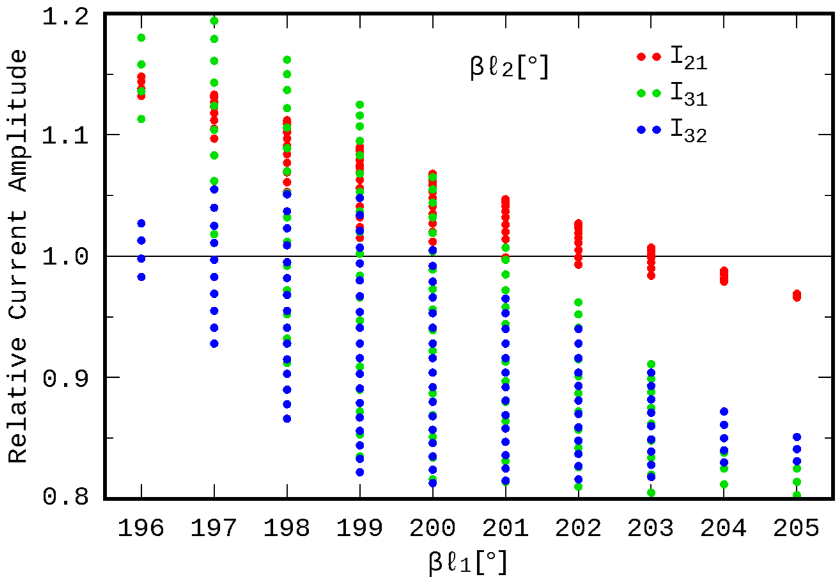

Fig. 16: Amplitude of current ratios for possible $\beta\ell_2$ values

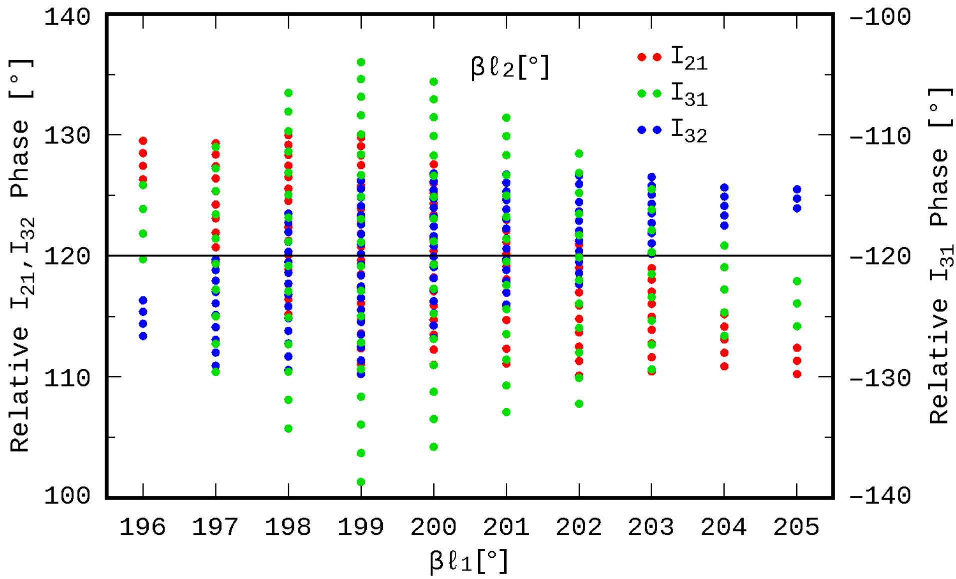

Fig. 17: Phase of current ratios for possible $\beta\ell_2$ values

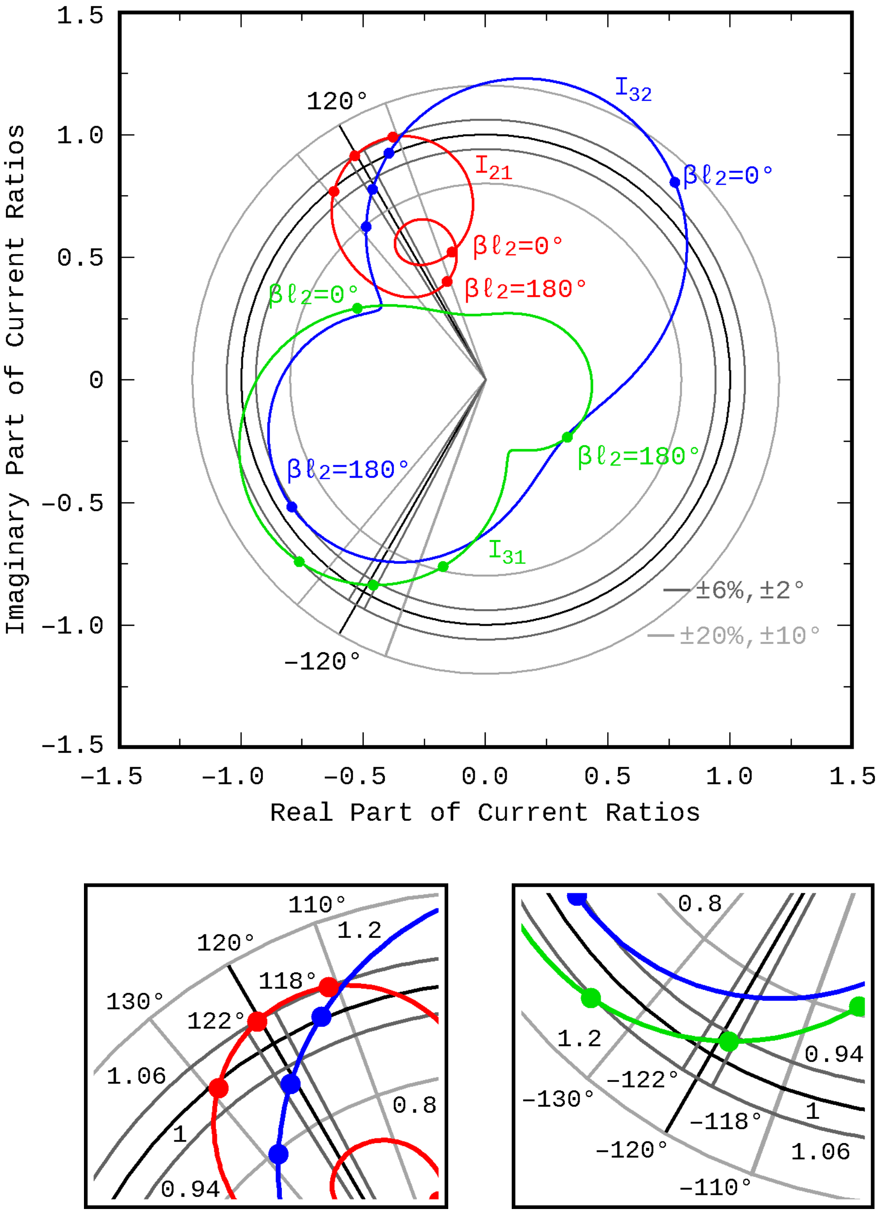

Fig. 18: Currents ratios versus $\beta\ell_2$ with $\beta\ell_1 = 200°$

Construction and Measurements

The designed EQ-ULA was simulated through the developed application and the [RichWire] simulation program, which is a fully analyzed, corrected and redeveloped edition of the original Moment Method thin-wire computer program [5], [6]. The number of segments for simulation was 72. The construction details and the measurement system are fully described in [2]. The [ANALYZE] application was used for the automated measurements [7], [8]. The simulation model and the constructed antenna are shown in Fig. 19 and in Fig. 20 respectively.

Notably, this array does not have any mechanical support other than its transmission line segments which have an appropriate form capable to achieve a clean self-standing array.

All the results for the 2D radiation pattern cuts by xOy, yOz, and zOx main-planes are shown in Fig. 21(a, b, c), both in Polar and Cartesian map. The scale of Cartesian chart was extended to –40 [dB] in order to include the small values of radiation intensity patterns. In Tab. 2 the maximum values per plane from analysis, simulation and measurement of the corresponding radiation patterns are shown.

Tab. 2: Maximum values

In [dB]	xOy	yOz	zOx
Analytical	–2.99	0.0	–49.23
Richwire	–2.21	0.0	–12.65
Measurement	–5.20	0.0	–6.7

Conclusion

In order to highlight the successful introduction of the idea of Electrical Quasi-Uniform Linear Array, EQ-ULA, using the dipole arrangement presented in this work, the input data and selected output results of [RadPat4W] application for a corresponding strict ULA [1], [5] are shown in Fig. 22.

Zero and maximum directions of ULA array factor were close enough to the required 45° and 135°, respectively. On the other hand, observing the radiation patterns in Fig. 21, especially that of yOz plane which represents the EQ-ULA array factor, there is indeed a zero in 45° from array axis ($\theta = 45°$, $\varphi = 90°$), whereas in 135° ($\theta = 45°$, $\varphi = 270°$) a maximum indeed exists with a small deviation in experimental results.

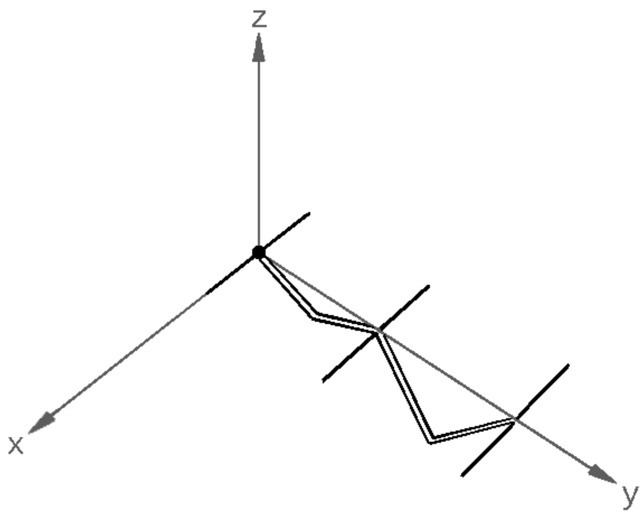

Fig. 19: The simulation model

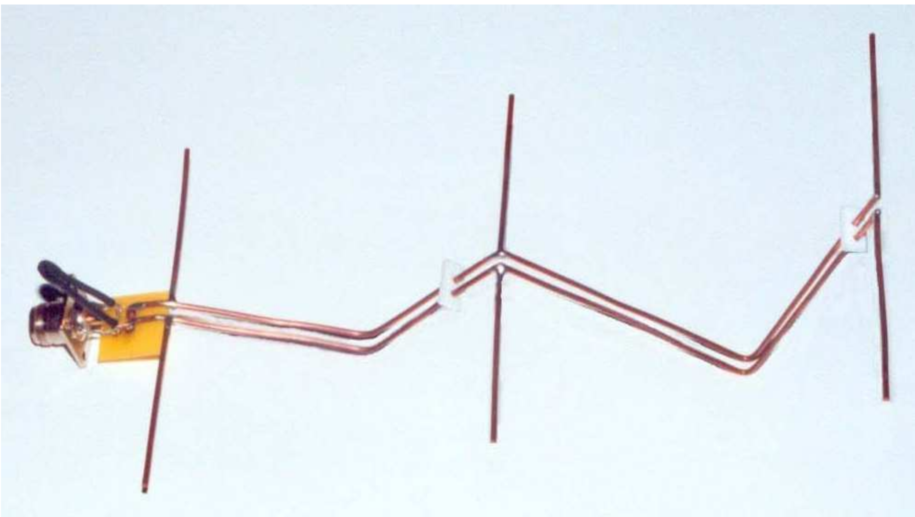

Fig. 20: The antenna array

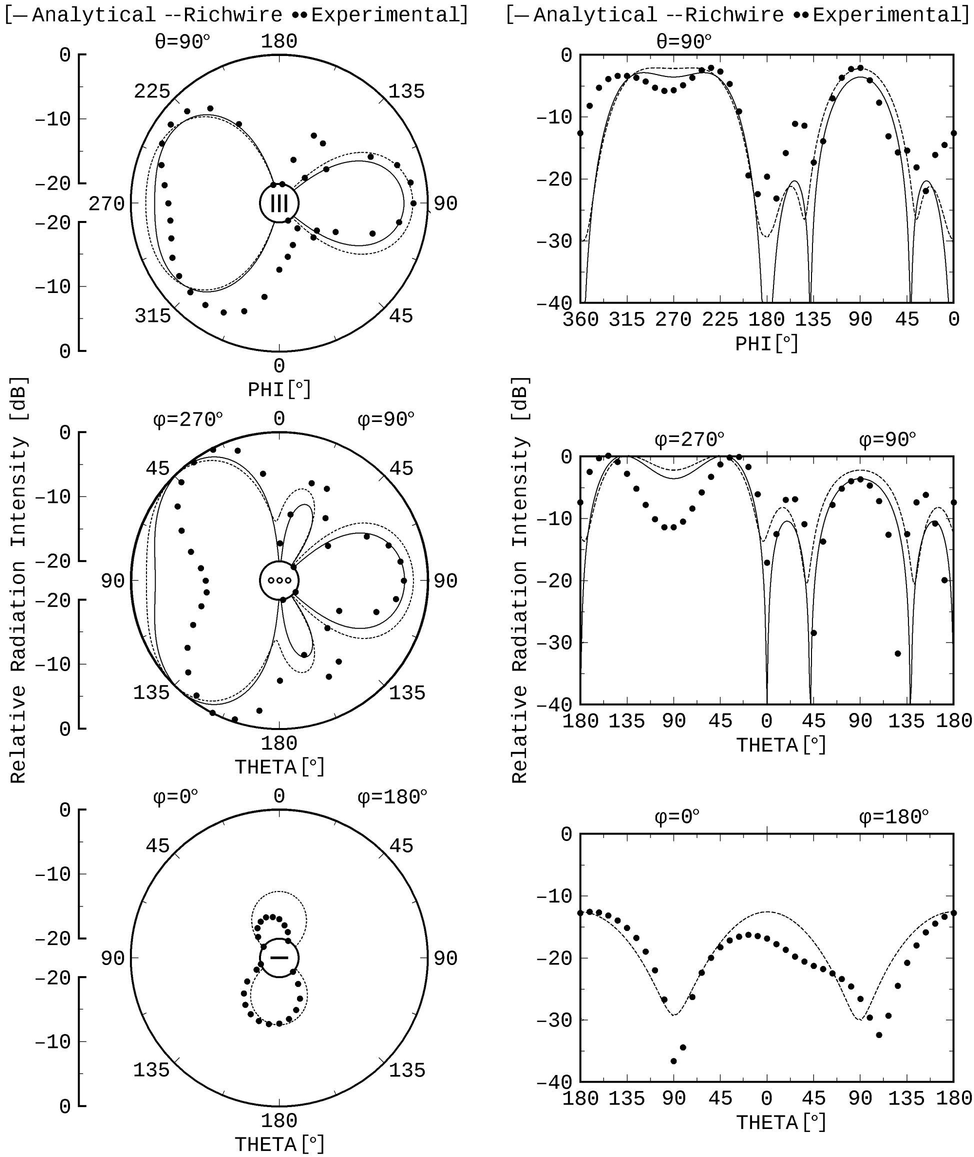

Fig. 21: Analysis, simulation and measurements for the experimental EQ-ULA array

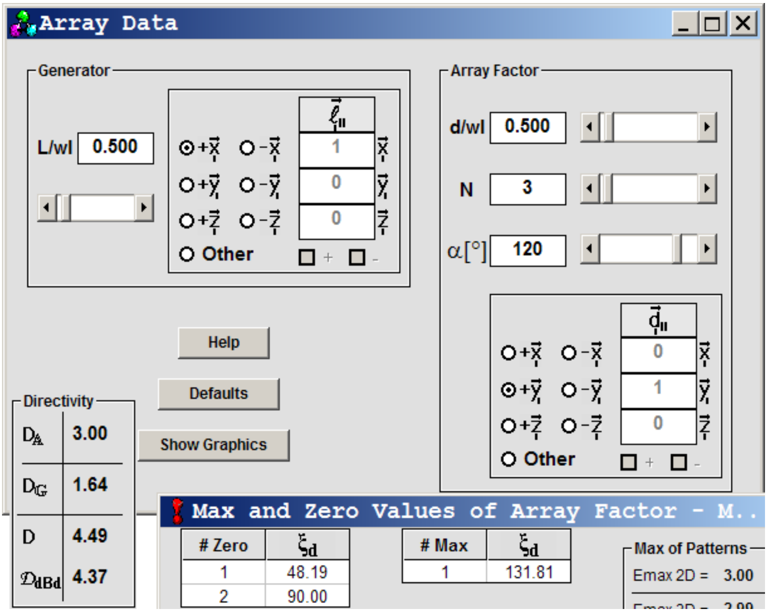

Fig. 22: Array Data of theoretical strict ULA

Fig. 23 contains a comparison regarding radiation patterns of the (i) designed and studied analytically EQ-ULA, (ii) theoretical strict ULA, (iii) simulation results, and (iv) measurements. Under the given measurement circumstances, it is obvious that, the experimental, computational, analytical and theoretical results were found to be in good agreement. The screen captures of the produced Virtual Reality radiation intensity patterns in dB for the array factor $\mathcal{A}$, the generator $\mathcal{G}$, and the dipole array $\mathcal{E}$ are given in Fig. 24.

Furthermore, according to the results of our ULA studies [1], if both directions of maximum of generator pattern and array factor coincide, then the antenna array directivity has directivity that it is at least as big as the maximum of the respecting two direcivities $D_{\mathcal{G}}$, $D_{\mathcal{A}}$. Since generator pattern is maximum everywhere on yOz plane and the array factor is maximum on a cone of 135° around its axis y, this condition is obviously satisfied. But $D_{\mathcal{G}} \approx 1.64$ and $D_{\mathcal{A}} = 3$ so $D \geq 3$. This prediction is successfully verified for (a) ULA which has $D \approx 4.49$, as it was computed by [RadPat4W], and (b) EQ-ULA which has D ≈ 4.22, as it results from [RichWire] simulation.

In this work the Quasi-Uniform characteristic, which was introduced regarding the electrical uniformity of an ULA, was experimentally proved to be a reliable solution to design and construct practical, non-trivial, linear uniform, end-fed, self-standing arrays, with a single driving point.

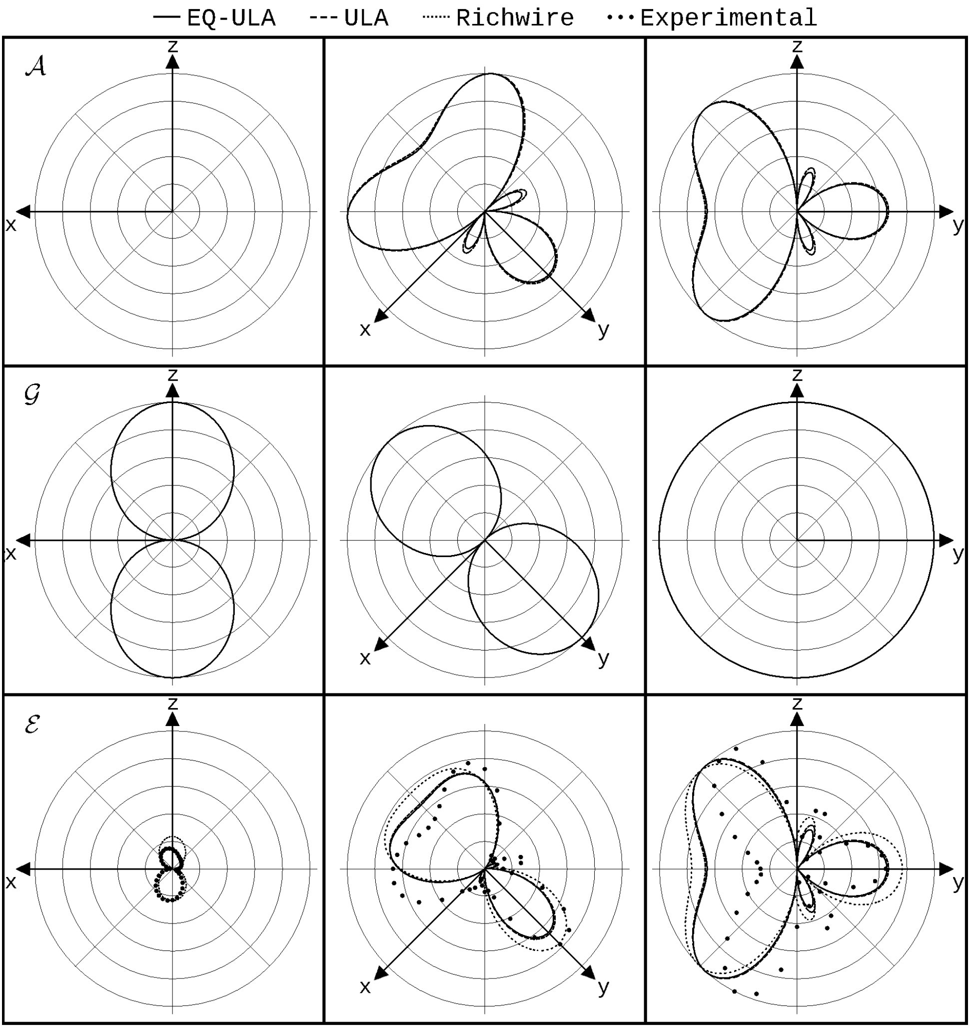

Fig. 23: Normalized 2D radiation patterns $\mathcal{A}$, $\mathcal{G}$, $\mathcal{E}$

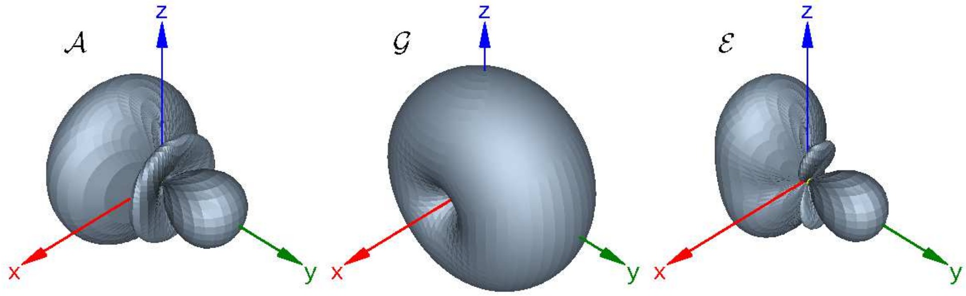

Fig. 24: Multiplication Principle: 3D patterns in dB [5]

References

[1] Zimourtopoulos P., "Antenna Notes 1999-, Antenna Design Notes 2000-(in Greek)
https://www.antennas.gr/antennanotes/

[2] Kondylis K.Th., Yannopoulou N.I., Zimourtopoulos P.E., "Self-Standing End-Fed Geometrically Uniform Linear Arrays: Analysis, Design, Construction, Measurements and FLOSS", FunkTechnikPlus # Journal, Issue 4, Year 1, 2014, pp. 43-52
https://www.otoiser.org/index.php/ftpj/article/download/41/36

[3] Kondylis K., "Standard Antenna Arrays", Master Thesis #1, ARG—Antennas Research Group, DUTh, 2002 (in Greek)
https://www.antennas.gr/theses/master/mt1-saa.pdf

[4] Kondylis K., "FLOSS for Self-Standing Linear Arrays of Dipoles"
https://arg.op4.eu/software/efa-eq-ula/eeu-src-exe-vr.7z
https://sourceforge.net/projects/antennas/files/efa-eq-ula/eeu-src-exe-vr.7z
https://www.antennas.gr/floss/EndFedArrays/

[5] Yannopoulou N., Zimourtopoulos P., "A FLOSS Tool for Antenna Radiation Patterns", Proceedings of 15th Conference on Microwave Techniques, COMITE 2010, Brno, Czech Republic, pp. 59-62

Yannopoulou N.I., Zimourtopoulos P.E., "Antenna Radiation Patterns: RadPat4W – FLOSS for MS Windows or Wine Linux", FunkTechnikPlus # Journal, Issue 5, Year 2, 2014, pp. 33-45
https://www.otoiser.org/index.php/ftpj/article/download/47/42

[6] Richmond J.H., "Computer program for thin-wire structures in a homogeneous conducting medium", Publication Year: 1974, NTRS-Report/Patent Number: NASA-CR-2399, ESL-2902-12, DocumentID: 19740020595
https://ntrs.nasa.gov/search.jsp?R=19740020595

[7] Yannopoulou N., Zimourtopoulos P., "ANALYZE: Automated Antenna Measurements, ver. 13", Antennas Research Group, 1993-2008

[8] Yannopoulou N., Zimourtopoulos P., "S-Parameter Uncertainties in Network Analyzer Measurements with Application to Antenna Patterns", Radioengineering, Vol. 17, No. 1, April 2008, pp. 1-8
https://www.radioeng.cz/fulltexts/2008/08_01_01_08.pdf

*Active Links: 30.09.2018

Previous Publication in FUNKTECHNIKPLUS # JOURNAL

"Measurement Uncertainty in Network Analyzers:
Differential Error DE Analysis of Error Models Part 5:
Step-by-Step Graphical Construction of
Complex DE Regions and Real DE Intervals",
Issue 16, pp. 7-25

*** About The Authors**

Konstantinos Kondylis, Issue 4, Year 1, p. 52
kkondylis@gmail.com

Nikolitsa Yannopoulou, Issue 9, Year 3, p. 390
yin@arg.op4.eu

Petros Zimourtopoulos, Issue 9, Year 3, p. 390
pez@arg.op4.eu